UNRAVELING THE GEOLOGIC HISTORY OF THE SOUTH POLE-AITKEN BASIN INTERIOR: A CASE STUDY OF THE BHABHA REGION USING MULTIPLE REMOTE SENSING DATASETS N.E. Petro[1], L.R. Ostrach[1], R. Clegg-Watkins[2,3], B.L. Jolliff[2], J.T.S. Cahill[4], P.O. Hayne[5], and S.C. Mest[3]; [1]NASA GSFC, [2]W.U. St. L., [3]PSI, [4]JHU/APL, [5]JPL, (Noah.E.Petro@nasa.gov)

Introduction: The enormous South Pole-Aitken Basin (SPA) represents a massive, yet unsampled terrane on the lunar farside [1]. A number of fundamental questions regarding lunar and Solar System evolution would be answered with a sample return from the basin interior. Highly desired samples foremost include impact melt material generated during the formation of SPA, and by subsequent small basins and large craters in the SPA interior to establish the SPA large impact chronology [2]. Basalts from mare and cryptomare deposits are also desired to test models of mantle heterogeneity and composition and timing of volcanism. Therefore, it is crucial that we unravel the geologic history of the basin interior and characterize the origins of various units within the basin. With current mission data, we can now use a wide array of remote sensing datasets in order to identify morphologic and compositional variations, as well as changes in the regolith over depths of centimeters to meters.

The existing geologic maps of the interior of SPA, based on Lunar Orbiter images [3, 4], while a key source for information on the relative stratigraphy of the basin, are in dire need of an update using modern datasets. Fortunately, geologic maps of the southern and western portions of the basin are being generated using LRO and Clementine data [5, 6]. These new mapping efforts show how the modern datasets revel new insights into SPA. Here, and in a companion abstract [7], we explore a region in Eastern SPA, near the center of the basin.

The Bhabha region (Fig. 1) contains the craters Bhabha and Bose, the western ejecta deposits from Stoney, as well as "Mafic Mound", a unique volcanic construct [8] as well as a number of small-scale volcanic deposits and likely cryptomare [9-11]. The contribution of basin ejecta to the region has previously been examined, showing that the regolith in this area is dominated by ancient SPA impact melt within ejecta deposits from nearby craters [12-14] that form the nonmare substrate.

Critical open questions regarding this region are: (1) What is the origin of the non-mare material within the region (SPA melt vs. cryptomare) and (2) What is the stratigraphy of the region, especially the sequence of ejecta deposits from these craters and other nearby craters? Recent datasets from the Lunar Reconnaissance Orbiter offer key insights into the variability and possible origin of surfaces in the region.

Mini-RF: Cahill et al. [15] showed that the average interior of SPA is distinct relative to the rocky interior of Orientale in the m-chi deconvolution (Fig.2), suggesting that the SPA regolith contains scatterers smaller than the wavelength of Mini-RF (12.6 cm) in the upper 1-1.5m, but it does contain some surface scatterers. Regional variations within the Bhabha region show near-surface rock enhancements around small, presumably fresh craters, as well as apparent enhancements in mare regions (NW and SW of Bhabha) and in the floor of Bhabha [9]. The putative cryptomare in the "Stoney Ejecta" region [10] lack any apparent rocks in the m-chi map (Fig. 2), suggesting a rock-poor regolith at the 12.6 cm scale.

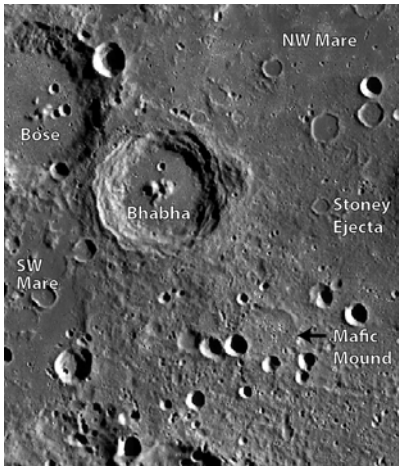

Figure 1. WAC morphology mosaic showing the Bhabha region (-52º to -60º latitude, and -170º to -158º) with key features identified. Mercator projection.

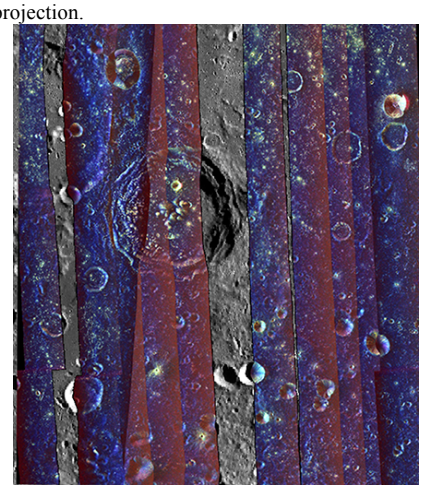

Figure 2. Mini-RF m-chi deconvolution map at 100 mpp of the Bhabha region [15]. Small-scale scatterers (<12.6cm) are more prevalent in proximal crater ejecta, crater walls and, apparently, in low-Ti mare regions that have a thinner regolith.

Diviner: Data from Diviner has proven to be valuable for producing map products that reveal regolith thermophysical variations (Figs. 3,4). These products highlight regional variations in regolith structure, revealing that small craters within mare regions and on the floors of Bhabha and Bose are enhanced in rocks (>~50 cm), and that there are no large, young [e.g., 16] craters in the region. Areas enhanced in rocks are almost

exclusively restricted to floors of large impact craters and mare deposits (NW/SW Mare in Fig. 1). As in Fig. 2, the putative cryptomare region (within the Stoney Ejecta) appears to have a relatively thicker and rock free regolith.

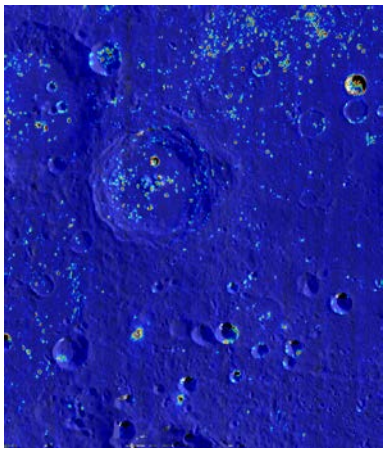

Figure 3. Diviner-derived rock abundance [17]. Small craters within the mare and floors of large craters (Fig. 1) have higher rock abundances, while areas in crater ejecta (Bhabha and Stoney) and in Mafic Mound [8] are relatively rock free (>~50 cm rock size).

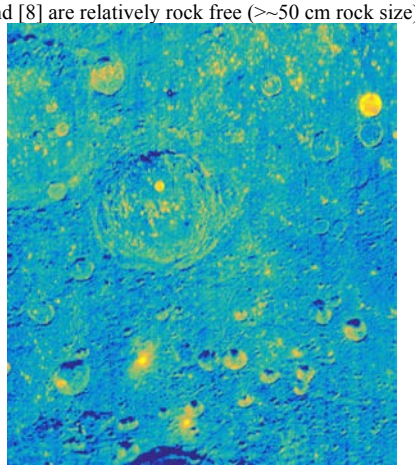

Figure 4. Diviner derived h-parameter map, representing the thickness (yellow=0cm, dark blue=20cm) of the low-density layer [18, 19]. Areas with little or no regolith (bright yellow) surround the few small, fresh craters, while areas of well-developed regolith (dark blue).

LROC WAC and NAC: The UV data from the LRO Wide Angle Camera has proven to be highly sensitive to space weathering as well as to surface composition [20]; a ratio of the 321nm/415nm bands reveals variations in ilmenite abundance and maturity. Areas in the northwest and west of the region appear to have a slightly lower ratio (Fig. 5), consistent with other mare areas, consistent the findings of Whitten and Head [9], but what is striking is the signature associated with ejecta from Stoney Crater (Fig.1), corresponding to a possible cryptomare deposit [7, 9, 10]. The unit lacks surface rocks (Fig.3), as seen in other mare and cryptomare deposits, and its origin needs to be further explored [7].

Narrow Angle Camera (NAC) images at the ~50cm scale reveal the rocks on surface and find that they are highly localized to the ejecta fields around fresh impact craters (Fig. 3). Topography derived from stereo observations is useful for meter-scale topographic analysis and to characterize morphologies that give rise to compositional variations and better evaluate mare, cryptomare, and nonmare surfaces. Additionally, an area of growing study is the use of multiple images at different phase angles covering the same area, which enable detailed photometric analysis [7].

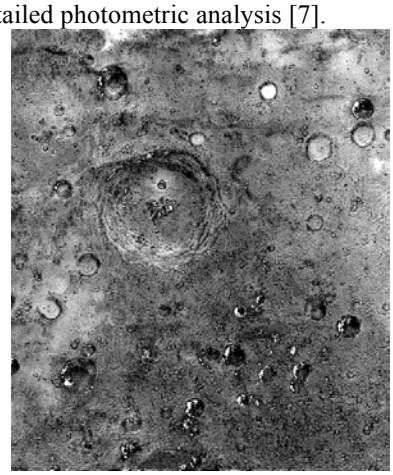

Figure 5. LROC WAC ratio image of the 321/415 bands [20]. Variations across the scene largely reflects composition, with some variations around smaller, fresh craters reflecting maturity.

Conclusions: LRO data, as well as complementary data from M^3 and the Kaguya Spectral Profiler [8, 21], continue to show the diversity within and uniqueness of SPA. Variations in buried and surface rocks are likely due to both the presence of mare basalts (or shallowly buried mare) as well as coherent impact melt beneath thin regolith on the floors of craters (Figs 2,3). Compositional variations across the region are linked to the presence of basalts and ancient volcanic constructs [7, 8, 10]. However, the origin of other mafic enhancements must be evaluated, with implications for the composition and proportion of mafic SPA-related impact melt. Integration of these datasets, as well as GRAIL gravity data [22], will lead to a better understanding of the origin of units within SPA. It is crucial to re-evaluate the ages of small units and craters within SPA, so that an improved stratigraphy of the interior can be generated.

References:[1] Jolliff, B., et al., (2000) *JGR*, 105, 4197-4216. [2] Hiesinger, H., et al., (2012) LPSC 43, [3] Stuart-Alexander, D. E., (1978) Geologic map I-1047. [4] Wilhelms, D. E., et al., (1979) Geologic map I-1162. [5] Mest, S. C., et al., (2015) LPSC 46, 2510. [6] Yingst, R. A., et al., (2015) LPSC 43 [7] Clegg-Watkins, R. N. and B. Jolliff, (2016), *These Proceedings*. [8] Moriarty, D. P. and C. M. Pieters, (2015) *GRL*, 42, 7907-7915. [9] Whitten, J. and J. W. Head, (2015) *PSS*, 106, 67-81. [10] Whitten, J. L. and J. W. Head, (2015) *Icarus*, 247, 150-171. [11] Petro, N. E., et al., (2011), doi:10.1130/2011.2477(1106). [12] Petro, N. E. and C. M. Pieters, (2004), doi:06010.01029/02003JE002182. [13] Petro, N. E. and B. L. Jolliff, (2011) LPSC 42, 2637. [14] Cohen, B. A. and R. F. Coker, (2010) *LPSC*, 41, 2475. [15] Cahill, J. T. S., et al., (2014) *Icarus*, 243, 173-190. [16] Ghent, R. R., et al., (2014) *Geology*, [17] Bandfield, J. L., et al., (2011) *JGR.*, 116, E00H02. [18] Bandfield, J. L., et al., (2014) *Icarus*, 231, 221-231. [19] Hayne, P., et al., (2013) Thermophysical Properties of the Lunar Surface from Diviner Observations, 15, 10871. [20] Denevi, B. W., et al., (2014) *JGR-P*, 119, 976-997. [21] Nakamura, R., et al., (2009) *GRL*, 36, L22202. [22] Petro, N. and B. Jolliff, (2013) LPSC 43, 2724.